

## FULL PAPER

# Reflectance Estimation for Proximity Sensing by Vision-Language Models: Utilizing Distributional Semantics for Low-Level Cognition in Robotics

Masashi Osada<sup>a</sup>, Gustavo A. Garcia Ricardez<sup>a,\*</sup>, Yosuke Suzuki<sup>b</sup>, and Tadahiro Taniguchi<sup>a</sup>

<sup>a</sup>College of Information Science and Engineering, Ritsumeikan University, Kusatsu, Japan

<sup>b</sup>College of Science and Engineering, Kanazawa University, Kanazawa, Japan

(v1.0 released March 2024)

While large language models (LLMs) and vision-language models (VLMs) have been increasingly used in robotics for problems requiring high-level cognition, their use for low-level cognition, such as interpreting sensor information, has not been sufficiently explored. In robotic grasping, proximity sensors are used to adjust the grasping pose before contact but the reflectance of the target objects significantly impacts the distance measured by the sensors. Therefore, estimating the reflectance of objects is crucial for successful grasping, which requires interpreting sensing information. Since LLMs embed human knowledge by keeping the relation between words as postulated by distributional semantics, it may be possible that LLMs can estimate reflectance from only object names without using any image input. Moreover, as VLMs are trained with image-text pairs, it may be possible that the latent structure of language positively affects the image-based reflectance estimation. In this paper, we verify that 1) LLMs such as GPT-3.5 and GPT-4 can estimate an object’s reflectance using only text as input; and 2) VLMs such as CLIP can increase their generalization capabilities and, consequently, achieve a higher accuracy in reflectance estimation from images. We evaluated the accuracy in reflectance estimation for unseen objects using LLMs with text input and VLMs with image input and compared them to image-only methods such as ResNet. As a result, GPT-4 achieved a mean error of 14.7%, lower than ResNet, even with the input being only text. Moreover, while CLIP achieved the lowest mean error of 11.8%, GPT-3.5 obtained 19.9%, a competitive result when compared to the image-only ResNet which achieved 17.8%. The results suggest that the distributional semantics in LLMs and VLMs increases their generalization capabilities and that the knowledge acquired by VLMs is positively affected by the latent structure of language.

**Keywords:** vision-language models, large language models, distributional semantics, low-level cognition in robotics, proximity sensors, reflectance estimation

## 1. Introduction

In recent years, large language models (LLMs) and vision-language models (VLMs) have been used in robotics for their high-level cognitive capabilities such as task planning and language understanding [1–4]. However, the usage of their low-level cognitive capabilities for real-world applications in the robotics field, such as sensor information interpretation, has not been thoroughly explored<sup>1</sup>. We argue that such low-level cognitive capabilities can be used in robotic grasping.

For a robot to grasp an object with various shapes and properties, it is possible to use proximity sensors to adjust the end effector pose before contact. However, as objects reflect the light emitted by the sensors according to their shape and properties, the sensors cannot accurately measure the distance unless such *reflectance* is known. Therefore, estimating the object’s reflectance is crucial for successful grasping and this requires interpreting the sensor information.

---

<sup>1</sup>We can find a few examples such as [5–7].

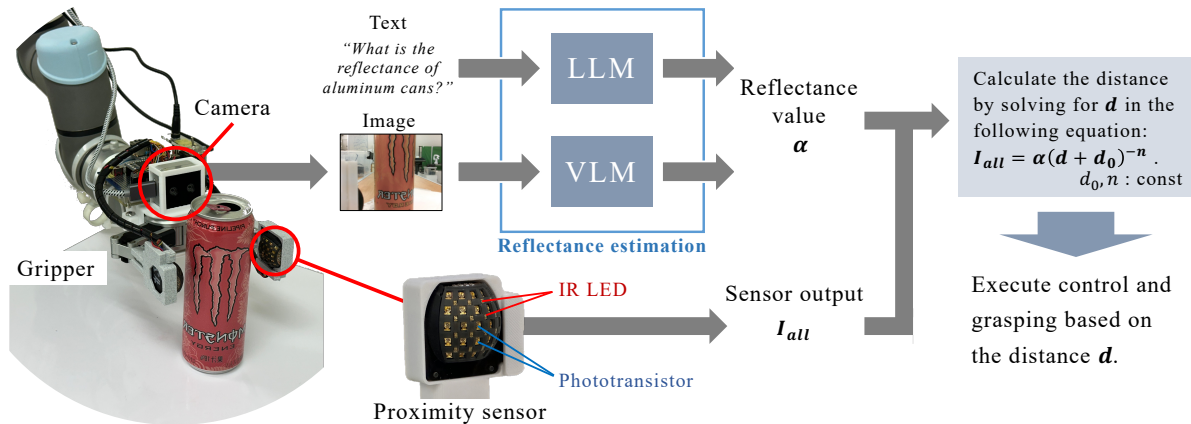


Figure 1. Reflectance estimation for proximity sensing. The LLMs and VLMs estimate the reflectance of objects whether from text (LLMs) or from images (VLMs). Together with the sensors’ output and the intrinsic parameters of the sensors, the estimated reflectance is used to measure the distance to target objects in preparation for grasping.

When attempting to estimate an object’s reflectance, conventional deep learning-based supervised learning systems are trained with labeled data for object categories and estimated values of their reflectance as teaching signals [8]. In such systems, the only clue for generalizing the learning results is the similarity of input images. Therefore, it is not possible to use the linguistic semantics of category names themselves for generalization.

In contrast, LLMs and VLMs implicitly form knowledge from the corpus based on distributional semantics [9], which could potentially be used for generalization. With LLMs and VLMs, it is possible to generalize knowledge about various vocabularies from the latent semantic relationships inherent in the language corpus [10, 11]. This generalization is not limited to the finite number of labels, which is often given in the training dataset of supervised learning-based estimation systems. Therefore, we focus on how LLMs and VLMs can leverage distributional semantics to interpret sensor information for low-level cognition in robotics.

More specifically, we aim to answer the following research questions:

**RQ1:** *Can LLMs estimate reflectance for proximity sensing just from the object name by using distributional semantics without any image features?*

**RQ2:** *Can the distributional semantics embedded in VLMs improve the performance of image-based reflectance estimation for proximity sensing with deep neural networks?*

In this paper, we demonstrate that even when estimating object-dependent reflectance, learning from the language corpus through the knowledge inherent in distributional semantics is useful, clarifying the advantages of utilizing distributional semantics in low-level cognition in robotics. We experimentally investigate the ability of LLMs and VLMs trained with only text and with text-image pairs to estimate the reflectance of objects and shed light on the capabilities of these models to exhibit low-level cognition. Furthermore, we use a method based on Contrastive Language-Image Pre-Training (CLIP) [12], a type of VLM that has been contrast-trained on a dataset consisting of an image and a string describing that image, and task it with reflectance estimation. Finally, we compare the accuracy of the estimated reflectance by LLMs and VLMs, and the conventional approach.

The main contributions of this paper are the following:

- We verify that distributional semantics in LLMs and VLMs increase their generalization capabilities, which in turn increases the accuracy of reflectance estimation.
- We verify that LLMs can estimate reflectance at a competitive level compared to conventional vision-based recognition methods without additional training using image data.

The rest of the paper is organized as follows. Section 2 introduces the related works. Section 3 details the evaluated methods. Section 4 presents the experimental results and offers a discussion. Finally, Section 5 concludes this paper.

## 2. Background

First, we introduce previous works on using sensing information before contact in the context of robot grasping. Here, we show the advantages of the type of sensors of our focus (i.e., proximity sensors), as well as relevant works demonstrating them. Second, we introduce the need for the interpretation of sensing information and argue that the generalization capabilities of LLMs and VLMs derived from distributional semantics can be used for such purpose.

### 2.1 *Robotic Grasping with Proximity Sensors*

On the one hand, for a robot to handle objects according to their various characteristics, it is desirable that the grasp pose is adjusted before contact. Proximity sensors can be used for this purpose [13]. These sensors that use optical reflection are compact and have a fast response time, which makes them suitable for mounting on fingertips and for providing feedback for motion control. Koyama et al. [14] have attached a sensor to the fingertip of the gripper to constantly measure the relative position of the gripper to the object, thereby enabling the robot to grasp objects according to their shape. The sensor attached to the fingertip of the gripper is a sensor that emits infrared light from the fingertip and receives the reflected light from the object, as shown in Fig. 1. This proximity sensor emits infrared light from the fingertip and calculates the distance based on the intensity of the infrared light reflected from the object.

In the proximity sensor used by Koyama et al., when the IR light emitted by the IR LED is reflected from an object, the phototransistor observes a reduced amount of IR light according to the distance between the object and the sensor and the properties of the object’s surface [14]. The phototransistor takes light as input and returns an electric current, and the degree of the current value depends on the amount of input light. Koyama et al. model the relationship between the obtained current value and distance as  $I_{\text{all}} = \alpha(d+d_0)^{-n}$ , where  $I_{\text{all}}$  is the current value obtained by combining the outputs of all phototransistors,  $\alpha$  is the reflectance of infrared light of each object, and  $d$  is the distance between the object and the sensor. In addition,  $d_0$  and  $n$  are intrinsic parameters. By attaching a sensor to the fingertip of the gripper and constantly measuring its relative position to the object, they have developed a method to control the movement of the fingertip for grasping according to the shape of the object and to carefully move the fingertip when the object and the fingertip are close to each other. Their work proposes a generic approach to grasping for object shape and softness.

Hirai et al. proposed a method that complements the image input from the camera with proximity information for areas that cannot be seen by the camera, and showed that object grasping can be performed faster and with a higher success rate [15]. In addition, Suzuki et al. proposed a method to constantly evaluate the stability of grasping by accurately grasping the shape of the object using the same sensor and showed that the success rate of grasping is improved for a variety of objects [16]. Hsiao et al. introduce proximity sensors integrated into the fingertips of a BarrettHand which, combined with a probabilistic model and a hierarchical reactive controller, improved grasping dynamically [17]. They utilize proximity sensors to make real-time adjustments to grasp points without the need for premature object contact or regrasping strategies.

The relationship between the intensity of the infrared light measured by the proximity sensor and the actual distance depends on the physical properties of the surface of each object and thus requires *a priori* information on the degree of reflection of the infrared light from each object. Konstantinova et al. propose a calibration method using RGB information obtained from a camera [18]. The accuracy of the proximity sensor is enhanced using the RGB information corresponding to the object to be grasped and then this data is used to obtain the correct calibration for the proximity sensor. Hasegawa et al. propose a method to estimate object-dependent parameters when used in conjunction with a reflectivity-independent Time-of-Flight sensor [19]. Their study fuses close-range and long-range sensors to overcome the limitations of each type of sensor.

From the model of Koyama et al., the equation of  $I_{\text{all}}$  indicates that the process of calculating the distance using the proximity sensor depends on the reflectance of the infrared light of the object of interest [14]. The calculation of the reflectance of each object requires that the distance between the sensor and the object be known, and it is difficult to accurately determine the reflectance for unknown objects. The method of Hirai et al. [15] uses manual input of the infrared reflectance of the target object, but this method is labor-intensive and may lack generalization performance for unknown objects.

To address this issue, Garcia et al. have developed a system that predicts the IR reflectance of a target object from image input using a CNN [8]. Specifically, the system uses representative CNNs, VGG16 [20] and ResNet101 [21], pre-trained on ImageNet, a large image dataset, and then performs fine-tuning to adapt the system to the task at hand. In the inference process, they assume that the reflectance of infrared light follows the category information of each object, and then calculate the expected reflectance of the object by summing the inferred likelihoods for each category with the weighted reflectance of the infrared light corresponding to each category. This means that the classification task is solved when the reflectance of each object calculated from the actual distance measured using the proximity sensor is considered as an independent category. This allows for efficient learning by taking into account the material of the object. While it is possible to learn efficiently considering the material of the object, it may be highly dependent on the data to be trained, and generalization performance for objects of unknown material may not be guaranteed.

## 2.2 *Language Models for Low-level Cognition*

On the other hand, even though LLMs have been attracting considerable attention in various fields, there is no satisfactory explanation for their extensive knowledge about our world and their ability to act appropriately, according to Mahowald et al. [22]. In general, the capabilities of LLMs are often discussed from a computational perspective, focusing on the transformer network structure [23]. However, it is known that language preserves the relationship between concepts represented by each word in a sequence, which is known as distributional semantics [9]. Distributional semantics studies the quantification and categorization of semantic similarities between linguistic items based on their distribution in language data [24].

The knowledge embedded in LLMs arises from distributional semantics, an intrinsic part of the language formed by human society, as explained from the perspective of collective predictive coding in symbol emergence in [25]. VLMs extend the principles of distributional semantics to multimodal contexts, where language is combined with visual information. By integrating distributional semantics with visual representations, VLMs can learn rich, generalized semantic knowledge that contains both linguistic and visual cues.

Gurnee and Tegmark demonstrated that LLMs learn representations of space and time across multiple scales [26]. Marjeh et al. investigate the extent to which LLMs can predict human sensory judgments [27]. The study reveals significant correlations between the model-generated judgments and human data across different domains, such as color and pitch, indicating the potential for extracting perceptual information from language.

Loyola et al. showed that there is significant correspondence between the human perceptual color space and the feature space found by language models [5]. Kawakita et al. compared the color similarity structures of humans (both color-neurotypical and color-atypical participants) with two GPT models, GPT-3.5 and GPT-4 [6]. The results indicated that the similarity structures of color-neurotypical humans align well with those of GPT-4, and to a lesser extent with GPT-3.5.

To predict the physical and electronic properties of crystalline solids from their text descriptions, LLM-Prop has been proposed [7]. Their method outperformed existing methods in predicting properties like band gap, unit cell volume, and more. This shows that LLMs are capable of predicting various physical properties of objects.

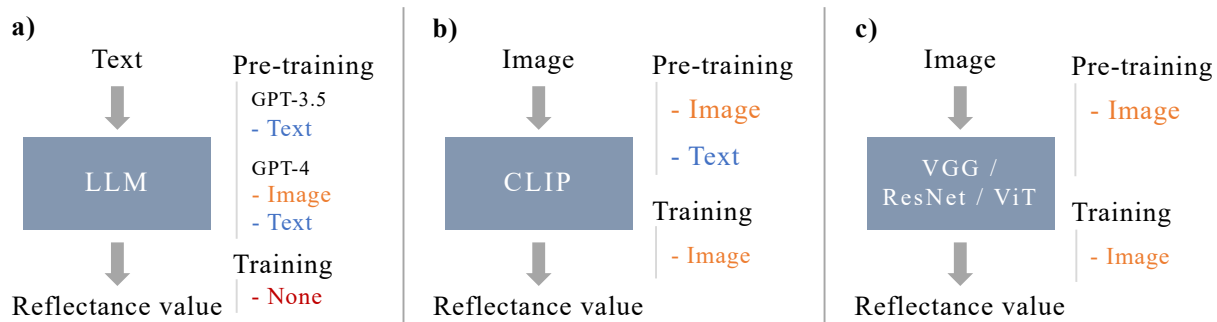


Figure 2. Overview of the three groups of methods used in the experiments. a) LLMs undergo pre-training that is either text-based or involves both text and images, without additional training. b) VLMs employ text and image pre-training, with additional image-based training. c) Compared methods use image-only pre-training and additional image training.

### 3. Methods

This section introduces the compared methods used for the reflectance estimation task. GPT-3.5 is a model trained only on text, while GPT-4 and CLIP are trained with images and text. As GPT-4 and CLIP are trained through different mechanisms, the former is considered an LLM, while the latter is considered a VLM. To clarify the effect of distributional semantics, we also compared the aforementioned methods to the image-only trained methods VGG16, ResNet101 and ViT-B/32 [28]. Fig. 2 shows a summary of the compared methods.

#### 3.1 GPT-3.5 and GPT-4

We use ChatGPT<sup>1</sup>, a chat service based on GPT-3.5 or GPT-4, as the LLMs. First, since the input to ChatGPT is a string, we manually assigned a string of one or two words that describe the images in the dataset.

The methodologies employed in this study are constructed through the application of Few-Shot Prompting and Chain-of-Thought techniques. Few-Shot Prompting refers to the method of providing a prompt with several example answers [10]. This approach, compared to Zero-Shot Prompting [29] where no examples are provided, offers stronger guidance through the prompt and has been reported to enhance the accuracy of outputs from LLMs across a variety of inference problems [30, 31]. Chain-of-Thought is a technique that involves explicitly or implicitly indicating the sequence of reasoning within the prompt, enabling more advanced inference than Few-Shot Prompting [32].

In this paper, we initially apply the concept of Few-Shot Prompting by providing the prompt with pairs consisting of a descriptive string for each image in the training dataset and the corresponding reflectance. Subsequently, based on the Chain-of-Thought approach, the method of thinking leading up to the answer is explicitly included in the prompt. First, the characteristics of light reflection on the object’s surface are inferred based on the object’s name. Next, by comparing the surface features and the sample reflectance provided in Few-Shot, a possible range of infrared reflectance is estimated. Finally, the most plausible value of infrared reflectance is provided as the answer. This method expects to obtain answers considering the material of the object. Additionally, this method can also predict the surface material implied by the object’s name implicitly; for example, from the name “Coffee,” it is experimentally confirmed that the surface is treated as equivalent to plastic if it is presumed to be in a plastic bottle, and the reflectance is answered accordingly. This leverages the inherent property of language models where the output of the LLM is influenced by the preceding text.

By doing this, we encourage the prediction of the reflectance values based on the material and reflective characteristics of each object. Finally, only the descriptive strings explaining each

<sup>1</sup>We use the versions gpt-3.5-turbo-0125 and gpt-4-0125-preview.

image in the test dataset are provided. Since Few-Shot Prompting initially indicates that the infrared reflectance follows the string representing the object, ChatGPT consequently outputs the reflectance for each string in the test dataset. A summarized example of the prompts used in this work is shown in Appendix B and in our repository<sup>2</sup>.

### 3.2 CLIP

The purpose of using CLIP in our research is based on the expectation that linguistic information retains details about light reflection, allowing for more accurate predictions than when using images alone. In other words, we expect the latent structure of language to affect the knowledge acquired by CLIP, as postulated by distributional semantics, leading to higher accuracy in the reflectance estimation from images.

CLIP [12] is a deep learning model that consists of two encoders: an image encoder and a text encoder. In the training process of CLIP, the visual information and linguistic information are contrasted using a dataset consisting of images and text strings describing the images, which are collected from a large number of images on the Web. Specifically, the image encoder and text encoder compute the cosine similarity of the extracted feature representations, and then proceed to increase the similarity if the input image/text pair is correct, and decrease the similarity if the pair is different. This makes it possible to extract common feature representations from images and text, respectively, so it is possible to consider the extraction of linguistic information from images or visual information from language.

The deep learning model used in the current work consists of a CLIP image encoder and two fully-connected layers. The number of units of all connected layers is set to 32 and 1, respectively. The second fully-connected layer has only one unit, so its function is to convert the output of the first layer (a 33-dimensional vector including bias) into a single number (a scalar). The learning process is performed in such a way that this scalar value corresponds to the desired reflectance. In general, when a pre-trained CNN is applied to individual tasks using a dataset such as ImageNet for category prediction, it is expected that the category prediction information obtained through pre-training will be useful for the desired inference. On the other hand, when CLIP is applied to individual tasks, it is expected that the target task can be represented in a more complex way because common feature representations are extracted from images and language.

Although there are various versions of CLIP depending on the model size and patch size, we use two versions: ResNet101 [21] and Vision Transformer (ViT-B/32) [28]. However, as a pre-training method for CLIP, we use the weights that have already been trained on 400 million pairs of images and text strings collected from the Web, as used in the original paper [12] by Alec et al., where they refer to it as WebImageText. We use the official implementation indicated in the same paper<sup>1</sup>, with the pre-trained weights of each model<sup>2</sup>. Furthermore, while CLIP consists of an image encoder and a text encoder, in this paper, we consider only the input of images and utilize the output from the image encoder exclusively. As CLIP acquires representations of features common to both language and images through Contrastive Learning, there is linguistic information implicitly related to the input image. In other words, the output of the image encoder for an image is pre-trained to be similar to the output of the text encoder for the text describing the same image, meaning that the output of the image encoder represents complex features with language as contextual information.

---

<sup>2</sup><https://github.com/Osada-M/ReflectanceEstimationByChatGPT>

<sup>1</sup><https://github.com/openai/CLIP>

<sup>2</sup>ViT-B/32: [openai/clip-vit-base-patch32](https://openai.com/clip-vit-base-patch32), ResNet101: [models/clip-resnet-101-visual-float16](https://openai.com/clip-resnet-101-visual-float16)



Figure 3. Objects used in the experiments. The objects on the left were used during the training phase, while those on the right were used during the testing phase. Besides regular objects, we also conducted experiments on irregular objects.

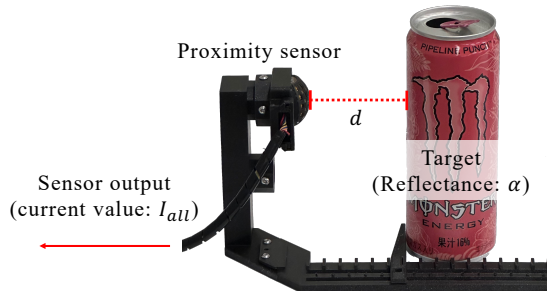


Figure 4. Setup to obtain the reflectance (ground truth) of objects at known distances. Given  $I_{all} = \alpha(d + d_0)^{-n}$ , where  $I_{all}$  is the current value obtained by combining the outputs of all phototransistor (measured) and  $d_0$  and  $n$  are intrinsic parameters (known), we can calculate the reflectance  $\alpha$  if the distance between the object and the sensor  $d$  is also known. We use the least squares method to obtain the ground truth value of  $\alpha$  by placing the object at various distances.

## 4. Experiments

We conduct experiments to estimate the reflectance of objects using GPT-3.5, GPT-4 and CLIP with ResNet101 and ViT-B/32. We evaluate the estimation accuracy by comparing the aforementioned methods to conventional image-only VGG16, ResNet101 and ViT-B/32. We set the loss function as the mean squared error, which is widely used in regression tasks.

### 4.1 Dataset

The dataset used in this paper consists of 324 pairs of images of 54 different objects taken from 6 different distances and the reflectance values of infrared light for each object. From these objects, 40 are treated as training data (*known objects*) and 14 as test data (*unseen objects*). Fig. 3 shows the objects in the training set and in the test set.

Besides conventional or regular objects, we also conducted experiments on irregular objects. This is because irregular objects are particularly challenging for proximity sensors because their non-uniform surface’s features and/or their transparency cause atypical readings from the sensors.

The true value of the reflectance of infrared light was calculated using a proximity sensor, and  $I_{all}$  was calculated from the relationship between the current output from the sensor when the sensor was moved between 5 and 30 [mm] at regular intervals from the object and the actual distance. The setup to collect such data is shown in Fig. 4, while examples of the proximity sensor output are shown in Appendix A.

### 4.2 Results

Table 1 shows the mean error between the ground truth and the predicted value of each method, while Fig. 5 shows also the statistical significance between the compared methods. Fig. 6 shows the results of reflectance estimation for the unseen objects (test set). It is worth mentioning that

\*:  $p < 0.05$ , \*\*:  $p < 0.01$

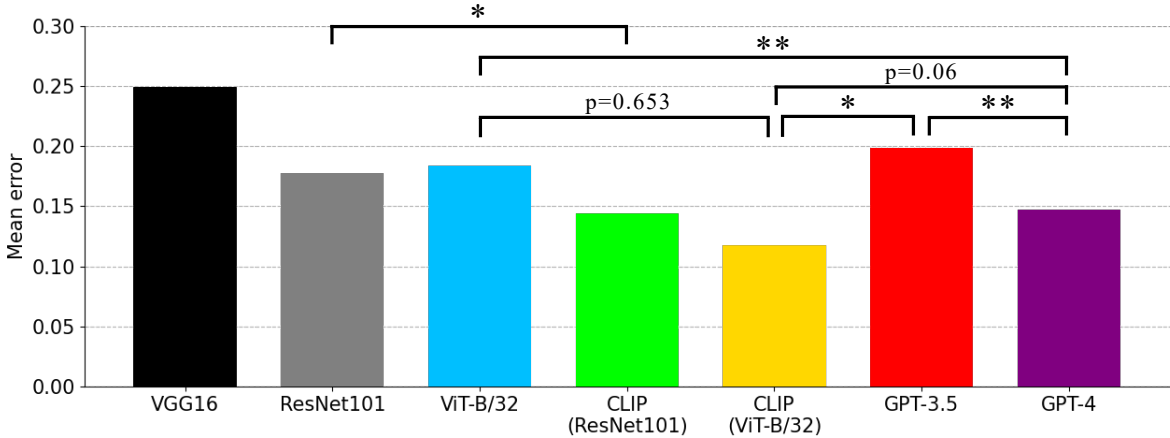


Figure 5. Mean error of the compared methods.

in the case of known objects (training set), as ChatGPT was given the true values directly in the prompts, the predictions for the training data returned exactly the true values (see Appendix C). Therefore, we focus only on evaluating the accuracy of unseen objects (test set).

Table 1 shows that the prediction using GPT-4 has higher accuracy compared to conventional methods, namely, VGG16, ResNet101 and ViT-B/32, which use solely images. When comparing GPT-3.5 and GPT-4, GPT-4 has higher accuracy. GPT-3.5 has higher accuracy than VGG16 and similar though inferior accuracy than ResNet101 and ViT-B/32. Although the structure and specific training processes of both models have not been disclosed at this time, the Technical Report [33] on GPT-4 shows that the number of parameters and training data for GPT-4 has increased significantly compared to GPT-3.5, and that GPT-4 is trained not only with language inputs but also with images.

The results show that the CLIP-based methods have a relatively high prediction accuracy for unseen objects compared to conventional methods. This is because the models can extract common information from images and language, allowing for more complex feature representations in the reflectance prediction model as a whole.

Fig. 6 shows that with the exception of the repellent, GPT methods achieve a relatively high accuracy. For the set of irregular objects, GPT-3.5 tends to underestimate the reflectance more than GPT-4. For transparent objects, most methods overestimate the reflectance, with only ResNet101 underestimating the reflectance of the marbles. Only in the case of the water bottle, conventional methods have relatively higher accuracy than CLIP-based methods, but lower accuracy than GPT methods.

Though CLIP (ViT-B/32) shows the highest accuracy, its mean error increases as the *difficulty* of the objects increase, from 6% for the regular objects, to 10% for the irregular objects and to 17% for the transparent objects. For regular and irregular non-transparent objects, GPT-4 seconds CLIP (ViT-B/32), while GPT-3.5 is second to last. However, GPT-3.5 surpasses GPT-4 for transparent objects by about 2%, the same margin that CLIP-based methods hold over GPT-3.5.

### 4.3 Discussion

In general, LLM/VLM methods outperformed the conventional approach; only GPT-3.5 was surpassed by the conventional ResNet101 and ViT-B/32. While the superior performance of GPT-4 over GPT-3.5 shows that the simultaneous learning of language and vision is crucial, GPT-3.5 showed competitive results compared to supervised methods, even without using any image data. This implies that the distributional semantics underlying LLMs trained only with text can be used to estimate reflectance, which is exacerbated by the contribution of text and

Table 1. Mean error of reflectance of infrared light

	Method	Pre-training dataset	Known objects	Unseen objects
Conventional	VGG16	ImageNet	$0.021 \pm 0.025$	$0.249 \pm 0.145$
	ResNet101	ImageNet	$0.008 \pm 0.008$	$0.178 \pm 0.143$
	ViT-B/32	ImageNet	$0.011 \pm 0.015$	$0.184 \pm 0.112$
VLM	CLIP (ResNet101)	WebImageText	<b><math>0.006 \pm 0.008</math></b>	$0.144 \pm 0.105$
	CLIP (ViT-B/32)	WebImageText	$0.008 \pm 0.010$	<b><math>0.118 \pm 0.094</math></b>
LLM	GPT-3.5	-	-	$0.199 \pm 0.255$
	GPT-4	-	-	$0.147 \pm 0.150$

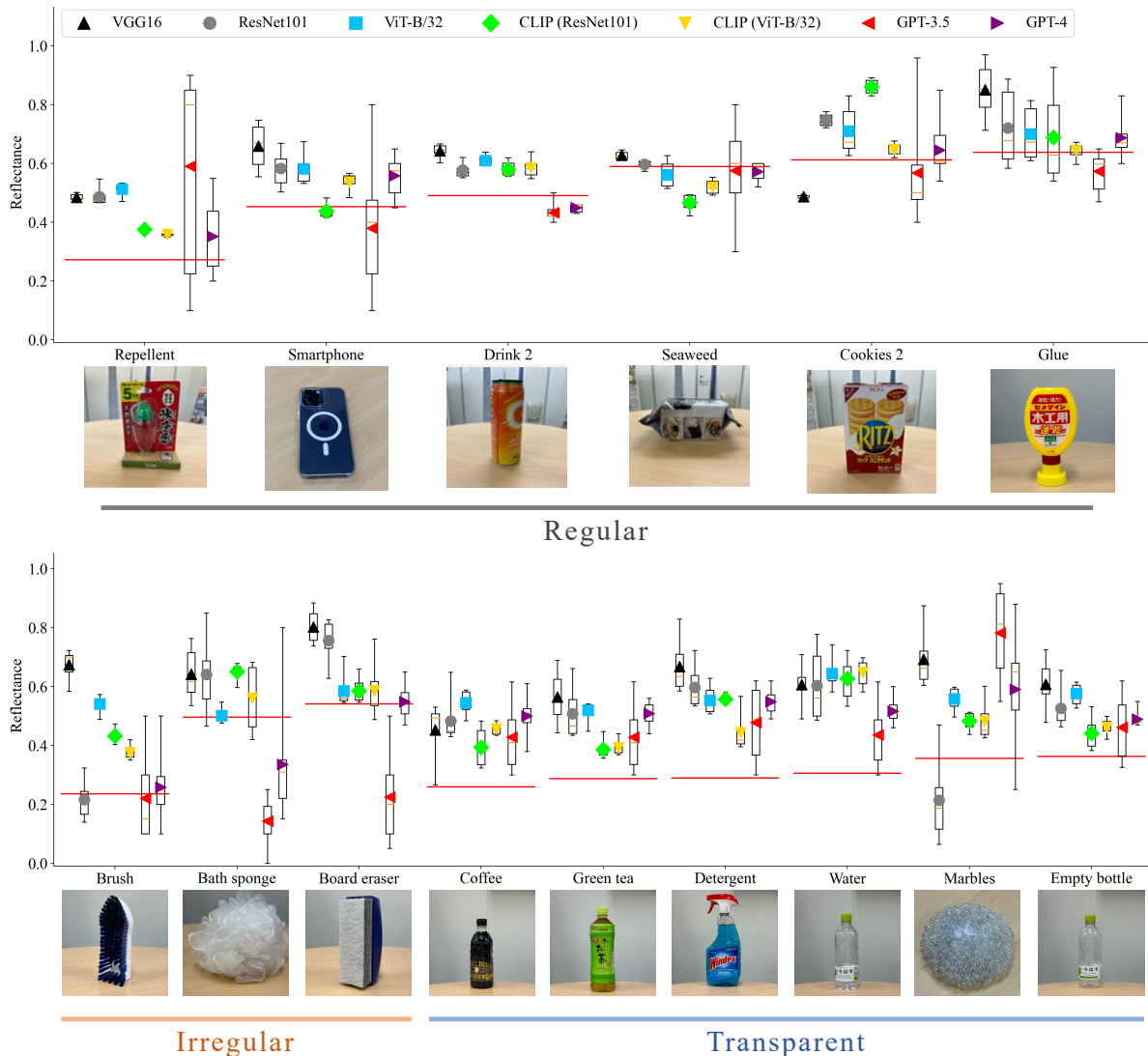


Figure 6. Estimated reflectance for unseen objects (test set).

image training in the case of GPT-4. (RQ1)

The effect of distributional semantics can also be observed when comparing the CLIP methods with their conventional counterpart, e.g., CLIP (ResNet101) and ResNet101. While being pre-trained on different datasets (ImageNet and WebImageText) could have an impact on the performance, one could assume that both datasets are sufficiently large and rich to make the (backbone) vision models equivalent. Then, the only salient difference is the text-image training of CLIP, which results in higher generalization in reflectance estimation. (RQ2)

ViT-B/32 results tend to be the average of the reflectance values, while GPT-3.5 shows high variability. On the other hand, CLIP methods displayed higher accuracy. This shows that not

using language information (image-only) leads to lower accuracy while relying only on language information for image-based tasks leads to more variable results. When using both image and language information, a higher accuracy can be obtained. (**RQ2**)

Regarding the results for transparent objects, LLM/VLM methods show high accuracy even though the prompt contained no explicit information about their transparency. This implies that the relationship between the objects and their physical properties is indeed embedded in the LLMs/VLMs, as distributional semantics suggests, and that such extrapolation capabilities increase their generalization capabilities. (**RQ1** and **RQ2**)

## 5. Conclusion

We experimentally verified that LLMs such as GPT-3.5 and GPT-4 can estimate an object’s reflectance using only text as input, and that VLMs such as CLIP can increase their generalization capabilities to achieve a higher accuracy in reflectance estimation from images. This suggests that the tacit knowledge derived from distributional semantics that these models possess can be used for low-level cognition in robotics. This was clarified in the paper from two perspectives. First, LLMs (GPT-3.5 and GPT-4) demonstrated a competitive performance when compared to existing methods through few-shot learning alone without using any image information. Second, VLMs (CLIP-based methods) achieved higher accuracy than baseline methods that learn from images alone. This means that learning from language and the obtained distributional semantics help to generalize the estimation of reflectance dependent on object classes from images.

Current work shows that language contributes to the generalization of reflectance estimation. However, as language is an abstraction in itself, this could cause a bias induced by implicit categorization, which could result in ignoring subtle differences in the objects. For example, *bottle(s)* can have a virtually infinite number of differences but they may be inadvertently categorized as a single type of objects. We plan to investigate to what extent this affects robotic grasping: while there may not be a significant effect on objects with monotonous surfaces, there may be significant effects on objects with particular variations.

Furthermore, the current work assumes a single reflectance value for the entire object but, in reality, objects can have multiple reflectance values across their surfaces. We plan to investigate if a higher level of detail can be obtained using LLMs and VLMs to create dense 3D maps of the objects’ reflectance.

Finally, as a similar approach can be followed for estimating other physical properties of objects, we plan to estimate the friction of the objects’ surfaces, which is crucial to calculate the force needed to grasp an object without letting it slip or crushing it.

## Acknowledgments

This work was supported by the Japan Science and Technology Agency (JST), Moonshot Research & Development Program, Grant Number JPMJMS2011.

## Authors

**Masashi Osada** received the B.Eng. degree in Information Science from Kanazawa Institute of Technology, Ishikawa, Japan, in 2023. He is currently pursuing a Master’s degree at Ritsumeikan University, Japan. His research interests include machine learning, particularly deep learning, and its real-world applications.

**Gustavo Alfonso Garcia Ricardez** received his MEng and PhD degrees from the Nara Institute of Science and Technology, Japan, in 2013 and 2016, respectively. He is currently

an Associate Professor at Ritsumeikan University, and a Research Advisor for Robotics Competitions at the Robotics Hub of Panasonic Corporation, where he leads numerous research projects and teams in international robotics competitions. His research interests include human-safe, efficient robot control, human-robot interaction, manipulation, and task planning.

**Yosuke Suzuki** received the B.Eng., M.Eng., and Ph.D degrees in engineering from the Tokyo Institute of Technology, Tokyo, Japan, in 2005, 2007, and 2010, respectively. He is currently an Assistant Professor with the Faculty of Mechanical Engineering, Institute of Science and Engineering, Kanazawa University, Kanazawa, Japan. His research interests include tactile and proximity sensors, robotic grasping, and distributed autonomous system.

**Tadahiro Taniguchi** received his MEng and PhD degrees from Kyoto University, in 2003 and 2006, respectively. From 2005 to 2008, he was a Japan Society for the Promotion of Science Research Fellow in the same university. From 2008 to 2010, he was an Assistant Professor at the Department of Human and Computer Intelligence, Ritsumeikan University. From 2010 to 2017, he was an Associate Professor in the same department. From 2015 to 2016, he was a Visiting Associate Professor at the Department of Electrical and Electronic Engineering, Imperial College London. Since 2017, he is a Professor at the Department of Information and Engineering, Ritsumeikan University, and a Visiting General Chief Scientist at the Technology Division of Panasonic Corporation. He has been engaged in research on machine learning, emergent systems, intelligent vehicle, and symbol emergence in robotics.

## References

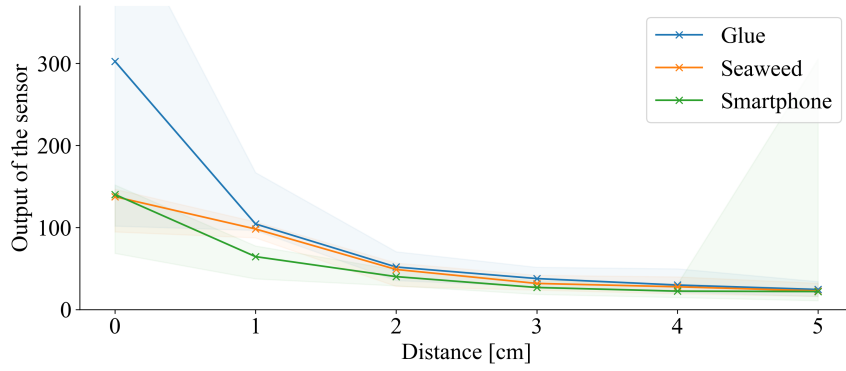
- [1] Shridhar M, Manuelli L, Fox D. CLIPort: What and where pathways for robotic manipulation. In: Faust A, Hsu D, Neumann G, editors. Proceedings of the 5th Conference on Robot Learning. Vol. 164 of Proceedings of Machine Learning Research. PMLR. 2022 08–11 Nov. p. 894–906.
- [2] Ahn M, Brohan A, Brown N, Chebotar Y, Cortes O, David B, Finn C, Fu C, Gopalakrishnan K, Hausman K, et al.. Do as I can, not as I say: Grounding language in robotic affordances. arXiv preprint arXiv:220401691. 2022;.
- [3] Khandelwal A, Weihs L, Mottaghi R, Kembhavi A. Simple but effective: CLIP embeddings for embodied AI. In: Proceedings of the IEEE/CVF Conference on Computer Vision and Pattern Recognition. 2022. p. 14829–14838.
- [4] Melnik A, Nandi GC, et al.. Exploring unseen environments with robots using large language and vision models through a procedurally generated 3D scene representation. arXiv preprint arXiv:240400318. 2024;.
- [5] Loyola P, Marrese-Taylor E, Hoyos-Idobro A. Perceptual structure in the absence of grounding for llms: The impact of abstractedness and subjectivity in color language. arXiv preprint arXiv:231113105. 2023;.
- [6] Kawakita G, Zeleznikow-Johnston A, Tsuchiya N, Oizumi M. Comparing color similarity structures between humans and llms via unsupervised alignment. 2023. 2308.04381.
- [7] Rubungo AN, Arnold C, Rand BP, Dieng AB. Llm-prop: Predicting physical and electronic properties of crystalline solids from their text descriptions. 2023. 2310.14029.
- [8] G A Garcia Ricardez, Z Yue, Y Suzuki, T Taniguchi. Reflectance Estimation for Pre-grasping Distance Measurement using RGB and Proximity Sensing. In: 2023 IEEE/SICE International Symposium on System Integration (SII). IEEE. 2023. p. 1–6.
- [9] Harris ZS. Distributional structure. In: Papers in Structural and Transformational Linguistics. Dordrecht: Springer Netherlands. 1970. p. 775–794.
- [10] Brown T, Mann B, Ryder N, Subbiah M, Kaplan JD, Dhariwal P, Neelakantan A, Shyam P, Sastry G, Askell A, Agarwal S, Herbert-Voss A, Krueger G, Henighan T, Child R, Ramesh A, Ziegler D, Wu J, Winter C, Hesse C, Chen M, Sigler E, Litwin M, Gray S, Chess B, Clark J, Berner C, McCandlish S, Radford A, Sutskever I, Amodei D. Language models are few-shot learners. In: Larochelle H, Ranzato

- M, Hadsell R, Balcan M, Lin H, editors. *Advances in Neural Information Processing Systems*. Vol. 33. Curran Associates, Inc.. 2020. p. 1877–1901.
- [11] Ramesh A, Pavlov M, Goh G, Gray S, Voss C, Radford A, Chen M, Sutskever I. Zero-shot text-to-image generation. In: *Int. Conf. on Machine Learning*. PMLR. 2021. p. 8821–8831.
- [12] Radford A, Kim JW, Hallacy C, Ramesh A, Goh G, Agarwal S, Sastry G, Askell A, Mishkin P, Clark J, et al.. Learning transferable visual models from natural language supervision. In: *Int. Conf. on Machine Learning*. PMLR. 2021. p. 8748–8763.
- [13] Navarro SE, Mühlbacher-Karrer S, Alagi H, Zangl H, Koyama K, Hein B, Duriez C, Smith JR. Proximity perception in human-centered robotics: A survey on sensing systems and applications. *IEEE Transactions on Robotics*. 2022;38(3):1599–1620.
- [14] Koyama K, Suzuki Y, Ming A, Shimojo M. Grasping control based on time-to-contact method for a robot hand equipped with proximity sensors on fingertips. In: *2015 IEEE/RSJ Int. Conf. on Intelligent Robots and Systems (IROS)*. IEEE. 2015. p. 504–510.
- [15] Hirai Y, Suzuki Y, Tsuji T, Watanabe T. High-speed and intelligent pre-grasp motion by a robotic hand equipped with hierarchical proximity sensors. In: *2018 IEEE/RSJ Int. Conf. on Intelligent Robots and Systems (IROS)*. IEEE. 2018. p. 7424–7431.
- [16] Suzuki Y, Yoshida R, Tsuji T, Nishimura T, Watanabe T. Grasping strategy for unknown objects based on real-time grasp-stability evaluation using proximity sensing. *IEEE Robotics and Automation Letters*. 2022;7(4):8643–8650.
- [17] Hsiao K, Nangeroni P, Huber M, Saxena A, Ng AY. Reactive grasping using optical proximity sensors. In: *2009 IEEE International Conference on Robotics and Automation*. 2009. p. 2098–2105.
- [18] Konstantinova J, Stilli A, Faragasso A, Althoefer K. Fingertip proximity sensor with realtime visual-based calibration. In: *2016 IEEE/RSJ International Conference on Intelligent Robots and Systems (IROS)*. 2016. p. 170–175.
- [19] Hasegawa S, Yamaguchi N, Okada K, Inaba M. Online acquisition of close-range proximity sensor models for precise object grasping and verification. *IEEE Robotics and Automation Letters*. 2020; 5(4):5993–6000.
- [20] Simonyan K, Zisserman A. Very deep convolutional networks for large-scale image recognition. *arXiv preprint arXiv:14091556*. 2014;.
- [21] He K, Zhang X, Ren S, Sun J. Deep residual learning for image recognition. In: *Proceedings of the IEEE Conference on Computer Vision and Pattern Recognition*. 2016. p. 770–778.
- [22] Mahowald K, Ivanova AA, Blank IA, Kanwisher N, Tenenbaum JB, Fedorenko E. Dissociating language and thought in large language models. 2023. 2301.06627.
- [23] Vaswani A, Shazeer N, Parmar N, Uszkoreit J, Jones L, Gomez AN, Kaiser Lu, Polosukhin I. Attention is all you need. In: Guyon I, Luxburg UV, Bengio S, Wallach H, Fergus R, Vishwanathan S, Garnett R, editors. *Advances in Neural Information Processing Systems*. Vol. 30. Curran Associates, Inc.. 2017. p. 6000–6010.
- [24] Lenci A. Distributional models of word meaning. *Annual Review of Linguistics*. 2018;4(Volume 4, 2018):151–171.
- [25] Taniguchi T. Collective predictive coding hypothesis: Symbol emergence as decentralized bayesian inference. *PsyArXiv preprint <https://osfio/preprints/psyarxiv/d2ty6>*. 2023;.
- [26] Gurnee W, Tegmark M. Language models represent space and time. 2024. 2310.02207.
- [27] Marjeh R, Sucholutsky I, van Rijn P, Jacoby N, Griffiths TL. Large language models predict human sensory judgments across six modalities. 2023. 2302.01308.
- [28] Dosovitskiy A, Beyer L, Kolesnikov A, Weissenborn D, Zhai X, Unterthiner T, Dehghani M, Minderer M, Heigold G, Gelly S, et al.. An image is worth 16x16 words: Transformers for image recognition at scale. *arXiv preprint arXiv:201011929*. 2020;.
- [29] Ling W, Yogatama D, Dyer C, Blunsom P. Program induction by rationale generation: Learning to solve and explain algebraic word problems. In: Barzilay R, Kan MY, editors. *Proceedings of the 55th Annual Meeting of the Association for Computational Linguistics (Volume 1: Long Papers)*. Vancouver, Canada: Association for Computational Linguistics. 2017 Jul. p. 158–167.
- [30] Min S, Lyu X, Holtzman A, Artetxe M, Lewis M, Hajishirzi H, Zettlemoyer L. Rethinking the role of demonstrations: What makes in-context learning work? In: Goldberg Y, Kozareva Z, Zhang Y, editors. *Proceedings of the 2022 Conference on Empirical Methods in Natural Language Processing*. Abu Dhabi, United Arab Emirates: Association for Computational Linguistics. 2022 Dec. p. 11048–11064.
- [31] Cobbe K, Kosaraju V, Bavarian M, Chen M, Jun H, Kaiser L, Plappert M, Tworek J, Hilton J,

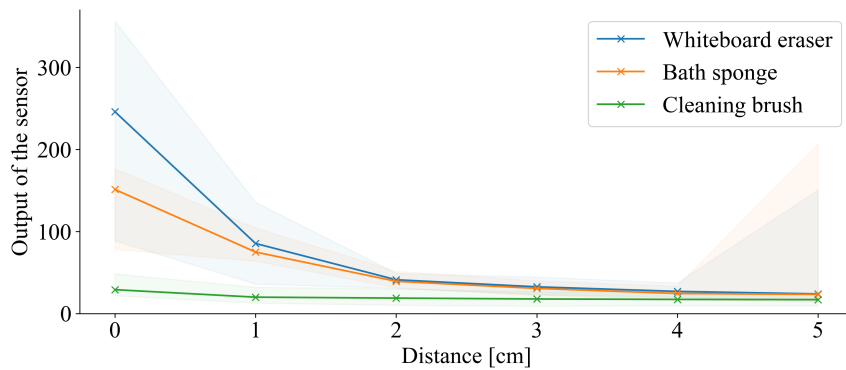
- Nakano R, Hesse C, Schulman J. Training verifiers to solve math word problems. 2021. 2110.14168.
- [32] Wei J, Wang X, Schuurmans D, Bosma M, Ichter B, Xia F, Chi E, Le Q, Zhou D. Chain-of-thought prompting elicits reasoning in large language models. 2023. 2201.11903.
- [33] OpenAI. GPT-4 Technical Report. arXiv preprint arXiv:230308774. 2023;.

## Appendix A. Proximity Sensor Output

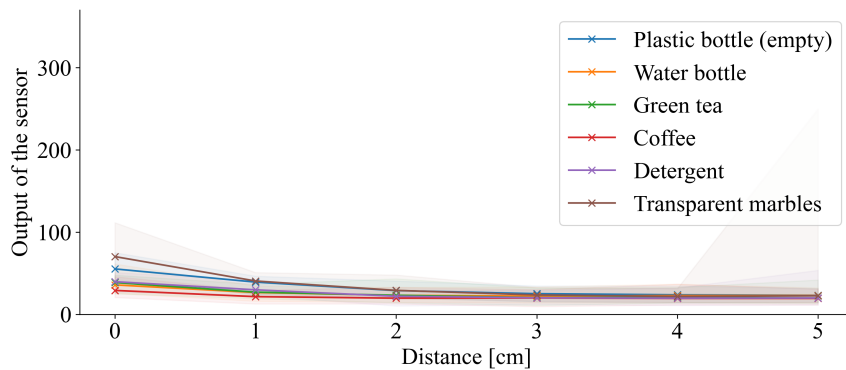
Fig. A1 shows the results of the measurements obtained with the proximity sensor. The vertical axis corresponds to  $I_{all}$ , which is the sum of the current from all the phototransistors in the proximity sensors.



(a) Regular objects.



(b) Irregular objects.



(c) Transparent objects.

Figure A1. Results of  $I_{all}$  for the calculation of the reflectance ground truth.

## Appendix B. Prompt to Estimate Reflectance with GPT-3.5 and GPT-4

The pseudocode of the prompts and an example of the replies are shown below. To improve readability, the prompt specifies that the output should be formatted as a table in markdown.

```
You are an expert in material properties. Your task is to determine the infrared reflectance of a given object. Please provide a single, reasonable value from the estimated range of infrared reflectance for each object. If your prediction is not conclusive, please output an approximate value as a guess. Note that the reflectivity of plastic bottles varies depending on their contents and labels.
```

```
Here are some example objects and their reflectance for reference:
```

```
dressings bottles [plastic, orange] : 0.326
dressings bottles [plastic, brown] : 0.327
dressings bottles [plastic, green] : 0.399
dressings bottles [plastic, yellow] : 0.403
...
```

```
---
```

```
User: get_reflectance(["energy drink", "yogurt"])
```

```
You:
```

```
|item|result|
|--|--|
|Name|energy drink|
|Reason|Aluminum is a metal, but its surface is printed with resin ink, which reflects light less than cardboard or mirrors. Since the reflectance of the chips tube is 0.684, the reflectance of an energy drink (aluminum can) is estimated to be 0.422.|
|**Response**|range: 0.41 - 0.46, prediction: **0.422**|
```

```
|item|result|
|--|--|
|Name|yogurt|
|Reason|Yogurt is a food product, but this is usually packaged in a plastic container. The yogurt container is considered less reflective than a similarly labeled plastic bottle. So, the reflectance of yogurt is greater than 0.616. On the other hand, it is white in color and will reflect relatively well. Therefore, we can expect it to be 0.75.|
|**Response**|range: 0.68 - 0.79, prediction: **0.762**|
```

### Appendix C. Reflectance Estimation for Known Objects

Fig. C1 shows the estimated reflectance for known objects (training set). In all cases, the image-only VGG16, ResNet101 and ViT-B/32 as well as the CLIP-based methods show a high accuracy on the training dataset. The results of GPT methods are omitted because the reference values for the training set were provided in the prompt, causing GPT methods to return exactly the same values.

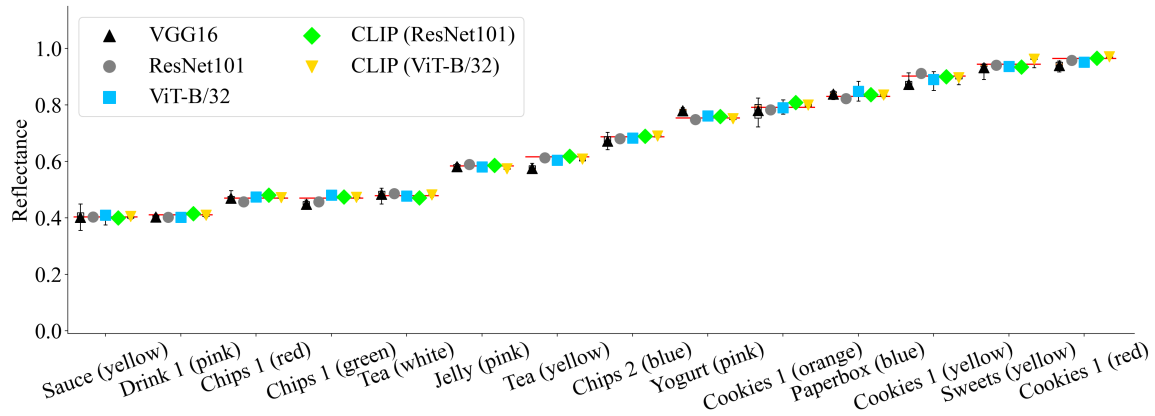


Figure C1. Estimated reflectance for known objects (training set).